Acta Neurochir (2010) 152:2037–2045
DOI 10.1007/s00701-010-0771-x

CLINICAL ARTICLE

Comparison of electrode location between immediate postoperative day and 6 months after bilateral subthalamic nucleus deep brain stimulation

Yong Hwy Kim · Hee Jin Kim · Cheolyoung Kim · Dong Gyu Kim · Beom Seok Jeon · Sun Ha Paek

Received: 6 May 2010 / Accepted: 9 August 2010 / Published online: 19 August 2010

Abstract
Objective We compared the electrode positions of subthalamic nucleus (STN) deep brain stimulation (DBS) estimated at the immediate postoperative period with those estimated 6 months after surgery.
Methods Brain CT scans were taken immediately and 6 months after bilateral STN DBS in 53 patients with Parkinson's disease. The two images were fused using the mutual information technique. The discrepancies of electrode positions in three coordinates were measured in the fused images, and the relationship with the pneumocephalus was evaluated.
Results The average discrepancy of *x*- and *y*-coordinates of electrode positions at the level of STN (3.5 mm below the anterior commissure–posterior commissure line) were 0.6±0.5 mm (range, 0~2.1 mm) and 1.0±0.8 mm (range, 0~5.2 mm), respectively. The average discrepancy of *z*-coordinates of the electrode tips of the fused images was 1.0±0.8 mm (range, 0.1~4.0 mm). The volume of pneumocephalus (range, 0~76 ml) was correlated with the *y*-coordinate discrepancies ($p<0.005$).
Conclusion The electrode positions in the immediate postoperative CT might have significant discrepancies with those in the CT taken at a stable period after STN DBS especially when there is a large amount of pneumocephalus.

Keywords Computed tomography · CSF leakage · Electrode position · Parkinson's disease · Pneumocephalus · STN DBS

Y. H. Kim · D. G. Kim · S. H. Paek (✉)
Department of Neurosurgery,
Seoul National University College of Medicine,
28 Yeongeon-dong Jongno-gu,
Seoul 110-744, South Korea
e-mail: paekshny@paran.com

H. J. Kim · B. S. Jeon (✉)
Department of Neurology,
Seoul National University College of Medicine,
28 Yeongeon-dong Jongno-gu,
Seoul 110-744, South Korea
e-mail: brain@snu.ac.kr

S. H. Paek
Hypoxic/Ischemia Disease Institute,
Seoul National University College of Medicine,
Seoul, Republic of Korea

S. H. Paek
Cancer Research Institute,
Seoul National University College of Medicine,
Seoul, Republic of Korea

D. G. Kim · B. S. Jeon · S. H. Paek
Clinical Research Institute, Seoul National University Hospital,
Seoul, Republic of Korea

C. Kim
Medical Imaging Laboratory, CyberMed, Inc.,
Seoul, Republic of Korea

Introduction

The subthalamic nucleus (STN) deep brain stimulation (DBS) has become one of the standard practices to alleviate intolerable symptoms and signs of the advanced Parkinson's disease (PD) [13, 14]. Due to the peculiar shape and size as well as the characteristic anatomical location of the STN, it is very difficult to precisely localize the electrodes and is painstaking to adjust the parameters of the pulse generator to best improve the parkinsonian symptoms and least provoke side effects without knowledge about anatomical location of the electrodes and contacts [2, 7, 18, 31].

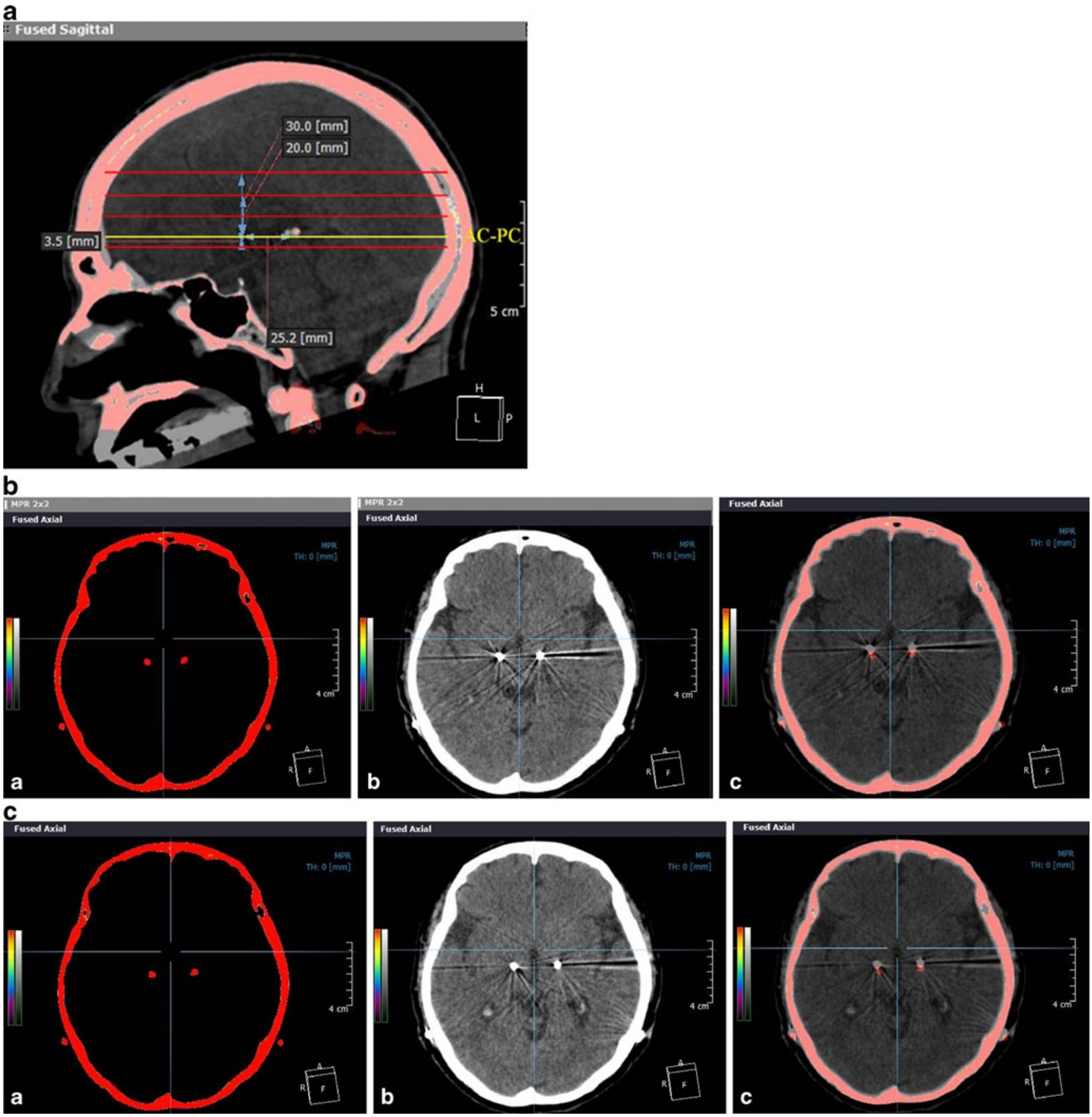

Fig. 1 The comparisons of electrode positions at five different sites between the immediate postoperative brain CT and the brain CT taken 6 months after bilateral STN DBS. After image fusion by using the mutual information technique, the marked discrepancy of electrode positions is shown distinctly. **a** The sagittal view of fused image of the immediate postoperative brain CT (*red*) and the brain CT taken 6 months after surgery showing the AC–PC line (*horizontal yellow line*), and the five levels are marked in *horizontal red lines*. **b** The axial view at the lowest level, 3.5 mm below the AC–PC line, where the subthalamic nucleus is well visualized along with the red nucleus and putamen. (*a*) Immediate postoperative brain CT in *red*. (*b*) Brain CT taken 6 months later. (*c*) Fused image of (*a*) and (*b*). **c** The axial view at the level of the AC–PC line, where the putamen is well visualized; (*a*) immediate postoperative brain CT in *red*; (*b*) brain CT taken 6 months after bilateral STN DBS; (*c*) fused image of (*a*) and (*b*). **d** The axial view at the level of 10 mm above the AC–PC line, where the septum pellucidum, thalamus, and the caudate nucleus, third ventricle, fornix are well visualized; (*a*) immediate postoperative brain CT in *red*; (*b*) brain CT taken 6 months after bilateral STN DBS; (**c**) fused image of (*a*) and (*b*). **e** The axial view at the level of 20 mm above the AC–PC line where the corpus callosum, caudate nucleus, and lateral ventricles are usually visible; (*a*) immediate postoperative brain CT in *red*; (*b*) brain CT taken 6 months after bilateral STN DBS; (*c*) fused image of (*a*) and (*b*). **f** The axial view at the level of 30 mm above the AC–PC line, where the lateral ventricle and centrum semiovale are visible; (*a*) the immediate postoperative brain CT in *red*; (*b*) the brain CT taken 6 months after bilateral STN DBS; (*c*) the fused image of (*a*) and (*b*)

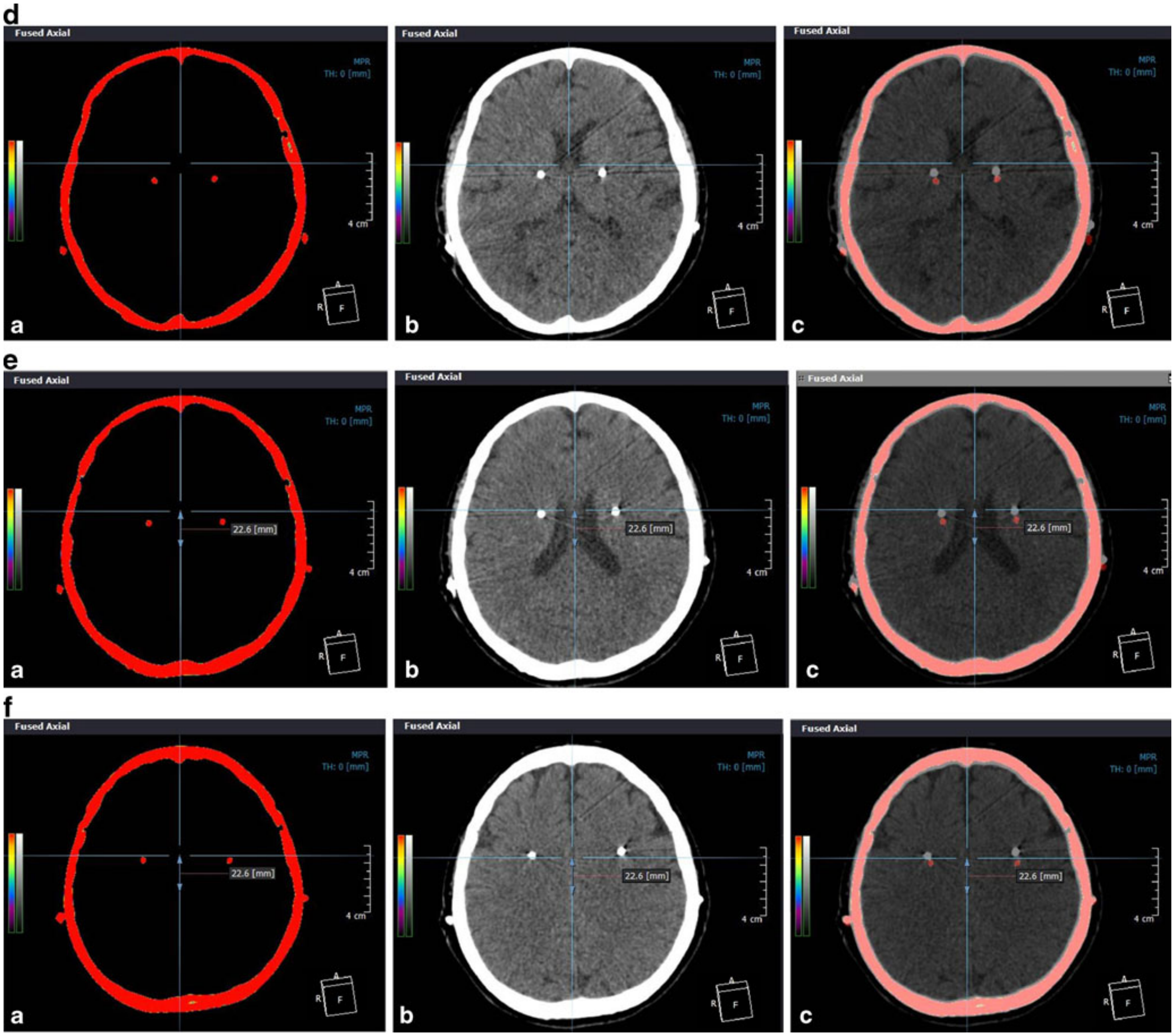

Fig. 1 (continued)

Therefore, the estimation of the electrode positions in relation with STN on the fused images of the preoperative brain MRI and postoperative brain MRI or CT by using fusion techniques deserves to be investigated to better adjust stimulation parameters after STN DBS surgery [9, 26, 28].

Regarding the image fusion, the lack of image distortion makes brain CT preferable to brain MRI for the estimation of the electrode positions after DBS surgery despite its poor details of anatomical structures [1, 22]. In the stance of such expectations, brain CT scans taken immediately or less than 1 week after DBS surgery has been frequently utilized to estimate the DBS electrode positions often fused with the images of preoperative CT or MRI in the literatures [3–6, 8, 16, 17, 23–25, 29, 31–34]. However, unexpected circumstances during the surgery such as the possible brain shift due to CSF leakage and electrode bendings might be concerns of the accuracy in the estimation of the electrode position based on the images taken at the short-term period after surgery. Until now, there has been little reported in the literature on the issue regarding the long-term validation of the estimated electrode positions from the postoperative brain CT scans taken immediately after surgery.

In order to validate the electrode positions estimated at the short-term period after surgery, we estimated the DBS electrode positions on the two brain CT scans taken immediately and 6 months after bilateral STN DBS surgery, and conducted an analysis of the discrepancies between them using image fusion techniques.

Methods

Patients and procedures

Fifty-three advanced PD patients, who had underwent bilateral STN DBS at the Movement Disorder Center of Seoul National University Hospital between March 2005 and October 2006, and had taken brain CT scans both at the immediate postoperative period and 6 months after surgery, were enrolled in this study. The male to female ratio of the patients was 20–33 with the mean age of 60.4±8.6 years (range, 29~75). This study was approved by the Institutional Review Board of SNUH. The surgical procedures were described elsewhere [11, 12]. On the day of the surgery, stereotactic MRI was performed for patients with the Leksell G frame (Elekta Instruments AB, Stockholm, Sweden), which was applied under local anesthesia. The stereotactic MRI was a 1.5-tesla MR imaging system (General Electric Medical Systems, Milwaukee, WI) using an eight-channel head coil with 2 mm contiguous axial proton density T2-weighted images and 1.5 mm interleaved contiguous axial T1-weighted images with and without contrast gadolinium enhancement. Surgery was performed under local anesthesia with utilization of the stereotactic coordinates in the Schaltenbrand Wahren human brain atlas and direct visualization of the STN in MRI by using Surgiplan® (Elekta Instruments AB, Stockholm, Sweden) as well as the microelectrode recording and macrostimulation. The entrance point into the skull was made 2–2.5 cm lateral to the midline at the level of the coronal suture, which provides an orthogonal approach. The angle of ring in the Leksell arc system (anteroposterior angle) was between 70° and 80°, and the angle of arc was between 85° and 95°. The quadripolar DBS electrode model 3389 (Medtronic Sofamor Danek, Minneapolis, MN, USA), with four platinum iridium cylindrical surfaces (1.27 mm diameter and 1.5 mm in length and 0.5 mm center-to-center separation) and Soletra model 7428 implanted pulse generator (Medtronic Neurological Division, Minneapolis, MN, USA) were implanted in a single session.

The 3-D spiral brain CT scans (64-channel Brilliance CT, Philips, Eindhoven, Netherlands) with a 1-mm slice thickness were performed both immediately and 6 months after bilateral STN DBS surgery. The amount of pneumocephalus in the brain CT taken at the immediate postoperative period after surgery was measured in each patient with OSIRIS program® (version 4.8; Service of Medical Informatics, Geneva University Hospital, Geneva, Switzerland).

Image fusions

The images of the two brain CT scans taken immediately and 6 months after DBS surgery was fused by using mutual information technique which was previously described elsewhere [10, 15]. We utilized the Lucion software (Cybermed, Seoul, Korea) based on the Windows operating system, allowing the simultaneous movement of the cursor in 3-D orthogonal planes. The fused image of the two 3-D spiral CT scans were aligned to anterior commissure (AC)–posterior commissure (PC) line. The midline of reformatted coronal images was also realigned to intersect the midsagittal plane for the correction of head-rotation error. On the reformatted axial view, the position of electrode center is localized as a dot by adjusting window level in the brain CT scans (Fig. 1).

The distance between the centers of electrodes from the two CT scans, and *x*-, *y*-coordinates of the centers of the electrodes and *z*-coordinates of the tips of the electrodes were measured from the fused images, and the average discrepancy was calculated (Fig. 1). The measurement was done at five different axial levels: 30 mm (centrum semiovale level), 20 mm (corpus callosum level), 10 mm (septum pellucidum level) above the level of the AC–PC line, at the level of the AC–PC line, and at the level of 3.5 mm below the AC–PC line (STN level). To minimize the discrepancy due to the observer, calculations were repeated by the same person twice with time interval of at

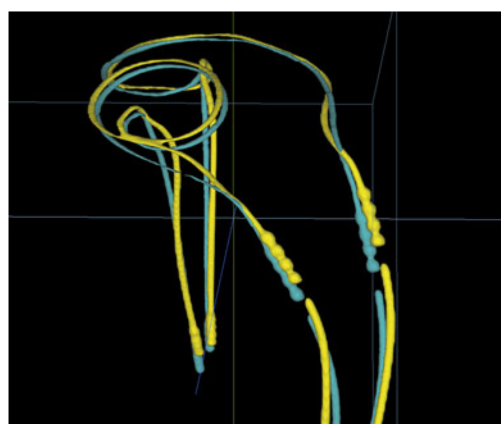

Fig. 2 Three-dimensional illustration of discrepancy of electrode position in the oblique lateral plane of the fused image of immediate postoperative brain CT and the brain CT taken 6 months after bilateral STN DBS surgery. The electrodes extracted from the immediate postoperative brain CT are *marked in yellow*, whereas the electrodes extracted from the brain CT taken 6 months after bilateral STN DBS are *marked in sky blue*. The marked discrepancy between the positions of both electrodes is shown. Especially, tips of both electrodes (*sky blue*) in the brain CT taken 6 months after bilateral STN DBS are more anteriorly and deeply positioned compared with those (*yellow*) in the immediate postoperative brain CT

Table 1 The discrepancies of *x*-coordinate between the electrodes on the immediate and 6 months postoperative brain CT scans according to the levels of measurement analyzed by the mixed model

		Left electrode			Right electrode		
		Estimate (mm)	Standard error (mm)	*p* value[a]	Estimate (mm)	Standard error (mm)	*p* value[a]
Level of measurement (from AC–PC line)	30 mm	0.9	0.1	<0.001	0.7	0.1	<0.001
	20 mm	0.8	0.1	<0.001	0.5	0.1	<0.001
	10 mm	0.6	0.1	<0.001	0.6	0.1	<0.001
	00 mm	0.5	0.1	<0.001	0.7	0.1	<0.001
	−3.5 mm	0.5	0.1	<0.001	0.7	0.1	<0.001

[a] $p<0.05$ means the distance was not the zero, statistically

least 1 week. The discrepant direction between two electrode on fused image in same coordinate, such as medial or lateral in *x*-coordinate and rostal or caudal in *z*-coordinate, was not considered in the measurement.

Statistical analysis

To assess the differences between the two kinds of imaging techniques, measurements of the *x*-, *y*-, and *z*-coordinates at each level were compared using mixed model. The correlation of the pneumocephalus with the discrepancies of the electrode positions was also evaluated using one-way analysis of variances (ANOVA) and simple correlation analysis. Statistical significance was set at *p* value less than 0.05. All statistical analyses were performed using SPSS ver 12.0 (SPSS Inc., Chicago, IL, USA)

Results

Discrepancy of the electrode positions

Total 106 electrodes in 53 patients treated with bilateral STN DBS were analyzed. Average distances between the electrodes on the immediate and 6 months postoperative brain CT scans were 1.8±1.3 mm (range, 0.1~7.3 mm) at 30 mm above the level of the AC–PC line, 1.6±1.3 mm (range, 0.1~6.2 mm) at 20 mm above the level of the AC–PC line, 1.5±1.0 mm (range, 0.1~5.0 mm) at 10 mm above the level of the AC–PC line, 1.4±0.9 mm (range, 0.1~4.4 mm) at the level of the AC–PC line, and 1.3±0.8 mm (range, 0.1~5.4 mm) at 3.5 mm below the level of the AC–PC line. The three-dimensional illustration of the average discrepancy of electrode positions in the oblique lateral plane of the fused image is shown (Fig. 2). The electrode tips on the postoperative 6 months brain CT were located more anteriorly and deeper compared with those on the immediate postoperative CT scan.

The average discrepancy of *x*-coordinates were 0.8±0.6 mm (mean±standard deviation, range, 0~3.1 mm) at 30 mm above the level of the AC–PC line, 0.7±0.5 mm (range, 0~2.4 mm) at 20 mm above the level of the AC–PC line, 0.6±0.5 mm (range, 0~2.6 mm) at 10 mm above the level of the AC–PC line, 0.6±0.5 mm (range, 0~2.8 mm) at the level of the AC–PC line, and 0.6±0.5 mm (range, 0~2.1 mm) at 3.5 mm below the level of the AC–PC line. The distance between two electrode on fused image was not zero, statistically ($p<0.001$). And, the side of electrode (left or right) had the interaction with the level of measurement in the statistical analysis ($p<0.001$). The estimate values and standard deviations of each levels were summarized in Table 1 and illustrated (Fig. 3).

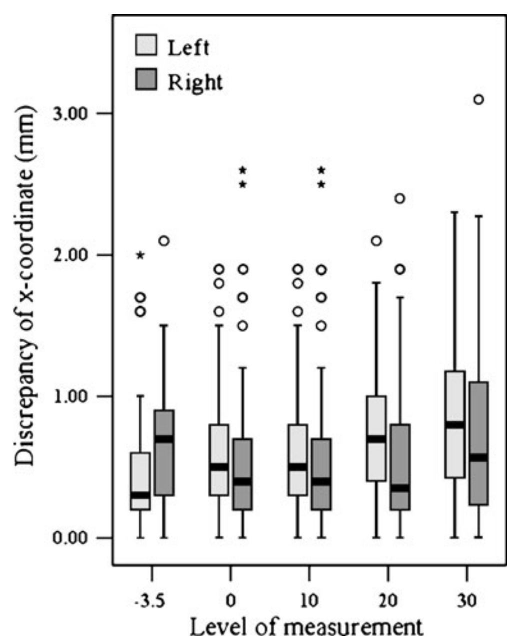

Fig. 3 Box plot of distance between two electrodes on axial fusion image. The distance was different according to the location of the electrode

Table 2 The discrepancy of the electrode position at five different sites of measurement between the immediate postoperative brain CT and the brain CT taken 6 months after bilateral STN DBS

Site of measurement	Distance between electrode on axial scan (mm)	Discrepancy of *x*-coordinate (mm)	Discrepancy of *y*-coordinate (mm)	Discrepancy of *z*-coordinate (mm)
30 mm above AC–PC line	1.8±1.3	0.8±0.6	1.4±1.3	–
20 mm above AC–PC line	1.6±1.3	0.7±0.5	1.3±1.4	–
10 mm above AC–PC line	1.5±1.0	0.6±0.5	1.2±1.0	–
AC–PC line	1.4±0.9	0.6±0.5	1.1±0.9	–
3.5 mm below AC–PC line	1.3±0.8	0.6±0.5	1.0±0.8	1.0±0.8

The discrepancies were more evident in the *y*-coordinate. The average discrepancy of *y*-coordinates were 1.4±1.3 mm (range, 0~7.2 mm), 1.3±1.4 mm (range, 0~6.0 mm), 1.2±1.0 mm (range, 0~4.9 mm), 1.1±0.9 mm (range, 0~4.4 mm), and 1.0±0.8 mm (range, 0~5.2 mm) at at 30, 20, and 10 mm above the level of the AC–PC line, same level of AC–PC line and 3.5 mm below AC–PC line, respectively. The distance of two electrode on fused image was not zero, statistically ($p<0.001$). In the statistical analysis, there was no significant interaction between the side of electrode (left or right) and level of measurement ($p=0.146$).

The discrepancy of electrode according to the *x*- and *y*-coordinate on the fused image and level of measurement (−3.5, 0, 10, 20, and 30 mm from AC–PC line) had the significant interaction. This meant that there was difference of discrepancy along the coordinates of electrode and level of measurement. Considering that the location of electrode on each level was the axial view of one electrode, it was easily expected.

The average discrepancy of *z*-coordinates of the tips of electrodes was 1.0±0.8 mm (range, 0.1~4.0 mm), and the side of electrodes did not influence the distance between two electrode on the fused image. Finally, there was significant difference in terms of distances between the electrodes on the immediate and 6 months postoperative brain CT. The distance between the electrode positions on the two CT scans was sub-analyzed into the *x*-, *y*-, and *z*-coordinates, and the values are showed in Table 2.

Influence of pneumocephalus on electrode localization

The average volume of pneumocephalus estimated in the immediate postoperative brain CT was 11.9±16.6 ml (0~76 ml). The patients were grouped into four according to the average volume of pneumocephalus; group 1, less than 10 ml (34 patients); group 2, between 10 and 20 ml (eight patients); group 3, between 20 and 30 ml (four patients); group 4, more than 30 ml (seven patients).

Table 3 Discrepancy of electrode position between immediate postoperative brain CT and brain CT taken 6 months after bilateral STN DBS according to the degree of postoperative pneumocephalus

Axis	Site of measurement	Group 1	Group 2	Group 3	Group 4	*p* value[a]
x-coordinates (mm)	30 mm above AC–PC line	0.8±0.7	0.8±0.6	0.8±0.5	0.7±0.5	0.977
	20 mm above AC–PC line	0.6±0.5	0.7±0.6	0.7±0.4	0.8±0.6	0.673
	10 mm above AC–PC line	0.5±0.5	0.9±0.7	0.5±0.3	0.7±0.5	0.038
	AC–PC line	0.5±0.4	0.9±0.8	0.5±0.4	0.7±0.5	0.023
	3.5 mm below AC–PC line	0.5±0.4	0.8±0.6	0.4±0.3	0.7±0.6	0.054
y-coordinates (mm)	30 mm above AC–PC line	0.8±0.7	1.7±0.7	2.4±1.4	3.3±1.9	<0.0001
	20 mm above AC–PC line	0.7±0.6	1.6±1.2	2.0±1.1	3.7±1.8	<0.0001
	10 mm above AC–PC line	0.8±0.5	1.6±1.0	1.9±1.1	2.8±1.4	<0.0001
	AC–PC line	0.8±0.5	1.4±0.8	1.5±0.8	2.1±1.4	<0.0001
	3.5 mm below AC–PC line	0.8±0.5	1.2±0.8	1.1±0.8	1.8±1.4	<0.0001
z-coordinate (mm)		1.0±0.8	1.0±1.0	1.1±0.9	1.0±0.8	0.893

[a] Statistical analysis according to the grade of pneumocephalus at each level using one-way ANOVA

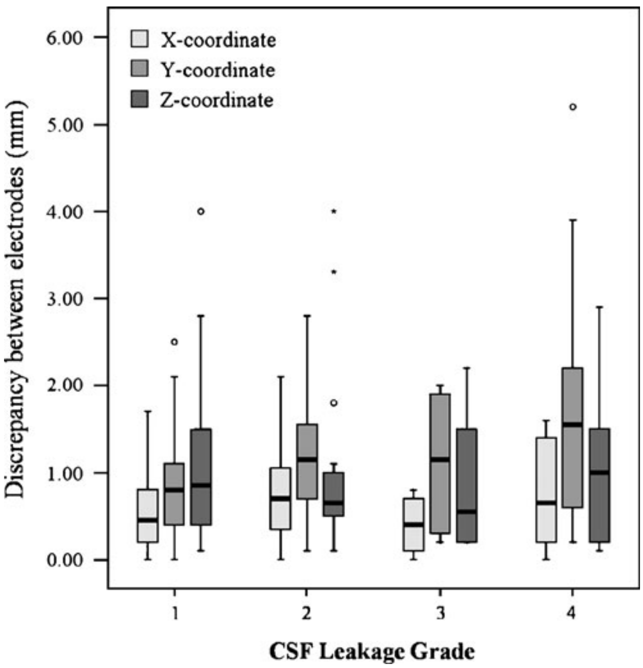

Fig. 4 Box plot of value of discrepancy of electrode positions between the immediate postoperative brain CT and the brain CT taken 6 months after bilateral STN DBS in three coordinates(x, y, and z) at the level of STN (at the level of 3.5 mm below AC–PC line) according to the grade of CSF leakage. Notably, the discrepancy of electrode positioning y-coordinate is correlated with the degree of CSF leakage

Statistic analysis showed a significant difference in the y-coordinates at all five levels ($p<0.001$, Table 3), and the average discrepancy of y-coordinates was most marked in group 4 and least in group 1. However, for the x- and z-coordinates, the difference was not statistically significant. The discrepancies in y-coordinates on all levels were also well correlated with the amount of pneumocephalus estimated at immediate postoperative brain CT (Fig. 4).

Discussion

The STN is the main target for DBS in Parkinson's disease [2, 13, 14]. Anatomical accuracy of stereotactic surgery was emphasized due to its small size and peculiar shape [2, 7, 31]. Despite the wide use of brain CT scan during the operation and immediately after the DBS surgery, unexpected circumstances during the surgery such as the possible brain shift due to CSF leakage and electrode bendings were not seriously considered in the estimation of electrode position shown in the brain CT at the immediate postoperative period after DBS surgeries.

In this study, we found that there was a significant discrepancy of the electrode positions between the immediate postoperative day and 6 months after surgery by estimating the electrode positions on the fused images of two brain CT scans using mutual information technique.

The migration of metallic material in the parenchyma of the central nervous system was reported in the literatures [21, 27]. And, the direction of movement coincided with the gravity or that of CSF flow. This feature was the evidence that the flow of CSF and gravitation is the main force affecting the intracranial location of the foreign body. The electrodes of DBS have different characteristics with the metallic material. First of all, they are anchored at cranium with cap of burr hole. Second, the flow of CSF could not force the electrode because the end point of electrode is located in the cerebral parenchyma and its trajectory does not pass through the ventricular system. Only sustained gravitation could influence its final location.

Table 4 Discrepancy of electrode position between brain CT taken at 1 and 3 months after bilateral STN DBS in comparison with the immediate postoperative CT in 15 patients

Axis	Site of measurement	Timing of CT		p value[a]
		1month	3months	
x-coordinates (mm)	30 mm above AC–PC line	0.7±0.6	0.8±0.7	0.346
	20 mm above AC–PC line	0.6±0.5	0.7±0.5	0.274
	10 mm above AC–PC line	0.4±0.4	0.4±0.3	0.879
	AC–PC line	0.4±0.3	0.4±0.3	0.153
	3.5 mm below AC–PC line	0.5±0.4	0.6±0.8	0.563
y-coordinates (mm)	30 mm above AC–PC line	1.0±0.9	0.9±0.8	0.484
	20 mm above AC–PC line	1.3±0.8	1.0±0.6	0.031
	10 mm above AC–PC line	1.3±0.6	1.3±0.5	0.284
	AC–PC line	1.2±0.5	1.3±0.5	0.503
	3.5 mm below AC–PC line	1.2±0.6	1.3±0.5	0.064
z-coordinates (mm)		0.4±0.4	0.5±0.5	0.693

[a] Statistical analysis between CT at each level using Mann–Whitney test

This study showed that the brain shift caused by the CSF leakage might influence the change of the electrode position on the chronological follow-up brain CT after bilateral STN DBS and the volume of pneumocephalus was mostly correlated with the *y*-coordinate discrepancies of electrode positions in the fused images. During surgery, patients positioned supine, and their neck was slightly flexed for comfort. After opening of dura, brain was shifted posterior according to the gravity and the shift will be proportional to the amount of leakage of CSF. This might have the *y*-coordinates mostly affected.

There were several trials to evaluate and correct the geographical error due to the brain shift during stereotactic brain surgery. Obuchi et al. reported the displacement of several important anatomical landmarks after DBS procedures based with postoperative MR [20]. The other study based on MR images, which were acquired on operation day and seventh postoperative day, showed that the intraoperative X-ray did not indicate the actual position in the target structure after brain shifts during surgery [19]. The study with follow-up CT also showed that the stereotactically implanted DBS electrodes were displaced upwardly with time, and it was significantly correlated with amount of air in the subdural space [30]. These studies calculated the displacement of electrode on the fusion image of preoperative and postoperative images; however, the fiducial points for the fusion of different images were not one of the brain structures but of the skull. As reported previously, the degree of shift is different according to the anatomical location [20]. Thus, the exact degree of displacement of DBS electrodes should be measured based on the fusion images according to the neural structures, which could be the standard in stereotactic surgery. So, authors measured the location of the electrode on the fusion images, which was aligned to AC–PC line because AC–PC line is the most important landmark in the planning of determining the location of STN and inserted DBS electrodes.

Based on our results, it is recommended that the DBS electrode position should be estimated in the brain CT scans taken at a certain period after DBS surgery when the possible brain shift had resolved. However, it is not clear when the appropriate time is to estimate the real position of the electrodes after surgery. To answer that question, we tried to compare the discrepancy of the center of electrodes between the immediate postoperative period, and 1 and 3 months after surgery in another 15 patients treated with STN DBS (Table 4). We found that there was no significant discrepancy of the center of electrodes estimated in the brain CT scans taken at between 1 and 3 months after surgery, whereas there was significant difference in the center of electrodes on the brain CT scans taken at between the immediate postoperative period and 1 month after surgery (Table 4). Therefore, we suggest that it is recommendable to confirm electrode position in the postoperative brain CT scans taken at least 1 month after surgery for the precise localization of the implanted DBS electrode.

Conclusion

We found that there was a significant discrepancy in the implanted electrode positions between the immediate postoperative period and 6 months after DBS surgery. The discrepancy was mostly obvious when the amount of pneumocephalus measured in the immediate postoperative CT was large. Finally, it seems that the stabilization of the electrode position may take at least 1 month following the surgery.

Acknowledgement This work was supported by a grant from Korea Healthcare Technology R&D project, Ministry for Health, Welfare and Family Affairs, Republic of Korea (A08-0663-A21724-08N1-000020B and A092052).

Conflicts of interest None.

References

1. Alexander E 3rd, Kooy HM, van Herk M, Schwartz M, Barnes PD, Tarbell N, Mulkern RV, Holupka EJ, Loeffler JS (1995) Magnetic resonance image-directed stereotactic neurosurgery: use of image fusion with computerized tomography to enhance spatial accuracy. J Neurosurg 83:271–276
2. Benabid AL, Chabardes S, Mitrofanis J, Pollak P (2009) Deep brain stimulation of the subthalamic nucleus for the treatment of Parkinson's disease. Lancet Neurol 8:67–81
3. Bittar RG, Burn SC, Bain PG, Owen SL, Joint C, Shlugman D, Aziz TZ (2005) Deep brain stimulation for movement disorders and pain. J Clin Neurosci 12:457–463
4. Breit S, LeBas JF, Koudsie A, Schulz J, Benazzouz A, Pollak P, Benabid AL (2006) Pretargeting for the implantation of stimulation electrodes into the subthalamic nucleus: a comparative study of magnetic resonance imaging and ventriculography. Neurosurgery 58:ONS83-95
5. Counelis GJ, Simuni T, Forman MS, Jaggi JL, Trojanowski JQ, Baltuch GH (2003) Bilateral subthalamic nucleus deep brain stimulation for advanced PD: correlation of intraoperative MER and postoperative MRI with neuropathological findings. Mov Disord 18:1062–1065
6. Coyne T, Silburn P, Cook R, Silberstein P, Mellick G, Sinclair F, Fracchia G, Wasson D, Stanwell P (2006) Rapid subthalamic nucleus deep brain stimulation lead placement utilising CT/MRI fusion, microelectrode recording and test stimulation. Acta Neurochir Suppl 99:49–50
7. Guehl D, Edwards R, Cuny E, Burbaud P, Rougier A, Modolo J, Beuter A (2007) Statistical determination of the optimal subthalamic nucleus stimulation site in patients with Parkinson disease. J Neurosurg 106:101–110
8. Hamel W, Fietzek U, Morsnowski A, Schrader B, Herzog J, Weinert D, Pfister G, Muller D, Volkmann J, Deuschl G, Mehdorn HM (2003) Deep brain stimulation of the subthalamic nucleus in

Parkinson's disease: evaluation of active electrode contacts. J Neurol Neurosurg Psychiatry 74:1036–1046
9. Holtzheimer PE 3rd, Roberts DW, Darcey TM (1999) Magnetic resonance imaging versus computed tomography for target localization in functional stereotactic neurosurgery. Neurosurgery 45:290–297, discussion 297–298
10. Ken S, Di Gennaro G, Giulietti G, Sebastiano F, De Carli D, Garreffa G, Colonnese C, Passariello R, Lotterie JA, Maraviglia B (2007) Quantitative evaluation for brain CT/MRI coregistration based on maximization of mutual information in patients with focal epilepsy investigated with subdural electrodes. Magn Reson Imaging 25:883–888
11. Kim HJ, Paek SH, Kim JY, Lee JY, Lim YH, Kim DG, Jeon BS (2009) Two-year follow-up on the effect of unilateral subthalamic deep brain stimulation in highly asymmetric Parkinson's disease. Mov Disord 24:329–335
12. Kim HJ, Paek SH, Kim JY, Lee JY, Lim YH, Kim MR, Kim DG, Jeon BS (2008) Chronic subthalamic deep brain stimulation improves pain in Parkinson disease. J Neurol 255:1889–1894
13. Limousin P, Krack P, Pollak P, Benazzouz A, Ardouin C, Hoffmann D, Benabid AL (1998) Electrical stimulation of the subthalamic nucleus in advanced Parkinson's disease. N Engl J Med 339:1105–1111
14. Limousin P, Pollak P, Benazzouz A, Hoffmann D, Le Bas JF, Broussolle E, Perret JE, Benabid AL (1995) Effect of parkinsonian signs and symptoms of bilateral subthalamic nucleus stimulation. Lancet 345:91–95
15. Maes F, Collignon A, Vandermeulen D, Marchal G, Suetens P (1997) Multimodality image registration by maximization of mutual information. IEEE Trans Med Imaging 16:187–198
16. McClelland S 3rd, Ford B, Senatus PB, Winfield LM, Du YE, Pullman SL, Yu Q, Frucht SJ, McKhann GM 2nd, Goodman RR (2005) Subthalamic stimulation for Parkinson disease: determination of electrode location necessary for clinical efficacy. Neurosurg Focus 19:E12
17. McClelland S 3rd, Senatus PB, Ford B, McKhann GM 2nd, Goodman RR (2007) Staged bilateral thalamic electrode implantation utilizing frameless stereotactic guidance. J Clin Neurosci 14:791–793
18. McClelland S 3rd, Vonsattel JP, Garcia RE, Amaya MD, Winfield LM, Pullman SL, Yu Q, Fahn S, Ford B, Goodman RR (2007) Relationship of clinical efficacy to postmortem-determined anatomic subthalamic stimulation in Parkinson syndrome. Clin Neuropathol 26:267–275
19. Miyagi Y, Shima F, Sasaki T (2007) Brain shift: an error factor during implantation of deep brain stimulation electrodes. J Neurosurg 107:989–997
20. Obuchi T, Katayama Y, Kobayashi K, Oshima H, Fukaya C, Yamamoto T (2008) Direction and predictive factors for the shift of brain structure during deep brain stimulation electrode implantation for advanced Parkinson's disease. Neuromodulation 11:302–310
21. Ott K, Tarlov E, Crowell R, Papadakis N (1976) Retained intracranial metallic foreign bodies. Report of two cases. J Neurosurg 44:80–83
22. Peters TM, Clark J, Pike B, Drangova M, Olivier A (1987) Stereotactic surgical planning with magnetic resonance imaging, digital subtraction angiography and computed tomography. Appl Neurophysiol 50:33–38
23. Pinto S, Le Bas JF, Castana L, Krack P, Pollak P, Benabid AL (2007) Comparison of two techniques to postoperatively localize the electrode contacts used for subthalamic nucleus stimulation. Neurosurgery 60:285–292, discussion 292–284
24. Pollo C, Vingerhoets F, Pralong E, Ghika J, Maeder P, Meuli R, Thiran JP, Villemure JG (2007) Localization of electrodes in the subthalamic nucleus on magnetic resonance imaging. J Neurosurg 106:36–44
25. Rampini PM, Locatelli M, Alimehmeti R, Tamma F, Caputo E, Priori A, Pesenti A, Rohr M, Egidi M (2003) Multiple sequential image-fusion and direct MRI localisation of the subthalamic nucleus for deep brain stimulation. J Neurosurg Sci 47:33–39
26. Saint-Cyr JA, Hoque T, Pereira LC, Dostrovsky JO, Hutchison WD, Mikulis DJ, Abosch A, Sime E, Lang AE, Lozano AM (2002) Localization of clinically effective stimulating electrodes in the human subthalamic nucleus on magnetic resonance imaging. J Neurosurg 97:1152–1166
27. Sorensen N, Krauss J (1991) Movement of hemostatic clips from the ventricles through the aqueduct to the lumbar spinal canal. Case report J Neurosurg 74:143–146
28. Starr PA, Vitek JL, Bakay RA (1998) Ablative surgery and deep brain stimulation for Parkinson's disease. Neurosurgery 43:989–1013, discussion 1013–1015
29. Tisch S, Zrinzo L, Limousin P, Bhatia KP, Quinn N, Ashkan K, Hariz M (2007) Effect of electrode contact location on clinical efficacy of pallidal deep brain stimulation in primary generalised dystonia. J Neurol Neurosurg Psychiatry 78:1314–1319
30. van den Munckhof P, Contarino MF, Bour LJ, Speelman JD, de Bie RM, Schuurman PR (2010) Postoperative curving and upward displacement of deep brain stimulation electrodes caused by brain shift. Neurosurgery 67:49–53, discussion 53–44
31. Vergani F, Landi A, Antonini A, Parolin M, Cilia R, Grimaldi M, Ferrarese C, Gaini SM, Sganzerla EP (2007) Anatomical identification of active contacts in subthalamic deep brain stimulation. Surg Neurol 67:140–146, discussion 146–147
32. Voges J, Volkmann J, Allert N, Lehrke R, Koulousakis A, Freund HJ, Sturm V (2002) Bilateral high-frequency stimulation in the subthalamic nucleus for the treatment of Parkinson disease: correlation of therapeutic effect with anatomical electrode position. J Neurosurg 96:269–279
33. Winkler D, Tittgemeyer M, Schwarz J, Preul C, Strecker K, Meixensberger J (2005) The first evaluation of brain shift during functional neurosurgery by deformation field analysis. J Neurol Neurosurg Psychiatry 76:1161–1163
34. Yelnik J, Damier P, Demeret S, Gervais D, Bardinet E, Bejjani BP, Francois C, Houeto JL, Arnule I, Dormont D, Galanaud D, Pidoux B, Cornu P, Agid Y (2003) Localization of stimulating electrodes in patients with Parkinson disease by using a three-dimensional atlas-magnetic resonance imaging coregistration method. J Neurosurg 99:89–99